Fe^{3+} distribution in oxidized olivine: A synchrotron micro-XANES study

M. DARBY DYAR,[1,*] JEREMY S. DELANEY,[2] STEVEN R. SUTTON,[3] AND MARTHA W. SCHAEFER[4]

[1]Department of Geography and Geology, Mount Holyoke College, 50 College Street, South Hadley, Massachusetts 01075, U.S.A.
[2]Department of Geological Sciences, Rutgers University, 610 Taylor Road, Piscataway, New Jersey 08854, U.S.A.
[3]Department of Geophysical Sciences & CARS, University of Chicago, Chicago Illinois 60637, U.S.A.
[4]Department of Geology and Geophysics, Yale University, New Haven, Connecticut 06520, U.S.A.

ABSTRACT

Synchrotron micro-XANES spectroscopy (SmX) is used to examine the amount and distribution of Fe^{2+} and Fe^{3+} in five samples of fayalite previously studied by Mössbauer spectroscopy. Rockport fayalite is homogeneous and the Fe in it is completely reduced. Olivine from Qianan is almost completely oxidized, and probably contains finely intergrown silica, laihunite, and hematite with hematite predominating. Pantelleria olivine has an oxidized rim around a reduced core, suggesting either a post-crystallization reaction with fayalite and oxygen going to laihunite and hematite or a change in prevailing oxidation during growth. The texture of olivine from the Mourne Mountains suggests exsolution from a fayalite-laihunite solid solution, based on the substitution of three Fe^{3+} atoms for two Fe^{2+} and one vacancy, that was stable at high temperature. Laihunite from the type locality (Lai-He village) shows 1–3 μm mottling between light and dark areas in backscatter images, but these areas cannot correspond to pure fayalite and laihunite exsolution because the bulk Fe^{3+}/ΣFe of such a combination would not correspond to the SmX value of 67% Fe^{3+}. Rather, the texture observed in backscatter is interpreted to represent alternating areas of magnetite-rich and laihunite-rich compositions with a similar (i.e., 67% Fe^{3+}/ΣFe) extent of oxidation.

INTRODUCTION

In 1934, Nikitin first reported the existence of a Fe^{3+}-rich olivine, which he called talasskite and later workers (Ginsburg et al. 1962) christened ferrifayalite; however these workers believed that ferrifayalite was a mixture of fayalite, hematite, and quartz. Subsequent discovery of the end-member Fe^{3+} olivine laihunite (Lai), or Fe^{2+}Fe$_2^{3+}$(SiO$_4$)$_2$, (Ferrifayalite Research Group 1986; Zhang et al. 1981) was also called ferrifayalite in deference to Ginsburg et al. (1962), but a later single-crystal refinement showed this is a single phase. Recently, the name laihunite was approved by the CNMMN to describe a distorted olivine structure consisting of M2 sites filled by Fe^{3+}, and M1 sites filled by Fe^{2+} and vacancies in alternate rows parallel to (001). The term "ferrifayalite" is now loosely used to describe samples with compositions representing solid solutions between laihunite and fayalite (although the physical scale of the solid solution is extremely variable), whereas the term "oxidized olivine" usually applies to Fe^{3+}-bearing olivine with other octahedral cations.

Numerous workers have synthesized (e.g., Iishi et al. 1989a, 1989b; Kondoh et al. 1985; Khisina et al. 1996) and characterized (e.g., Tamada et al. 1983; Shen et al. 1986; Banfield et al. 1990) olivine containing Fe^{3+}. Fe^{3+}/ΣFe was not directly measured, but it was inferred from vacancy distributions determined by TEM or related techniques. Yet, significant Fe^{3+} concentrations may occur in olivine but are not revealed by TEM because they are masked by Mg-Fe disorder (Janney and Banfield 1998).

Some oxidized olivine (Ol) has a significantly different struc-ture than laihunite and is actually composed of multiple phases (Banfield et al. 1990; Janney and Banfield 1998). For example, Kitamura et al. (1984) reported interstratifications of OH$^-$ monolayers with olivine (resulting in humite-like layers) in oxidized olivine from mantle kimberlite. TEM on defects in partially oxidized (up to 6% Fe^{3+}/ΣFe) metasomatized mantle peridotitic olivine (Banfield et al. 1992) shows intergrowths of olivine and a laihunite-like material. Oxidation of Fa$_{11}$ olivine results in formation of "ferriolivine" planes plus magnesioferrite and magnetite (Mgt) (Khisina et al. 1995), whereas olivine oxidized in alkaline environments results in intergrowths of hematite (Hem) and amorphous silica, and oxidation in an acidic environment produces Ol + Hem + Lai (Iishi et al. 1997). These studies confirm the microscale interrelationships between oxides, silica, humite, vacancy-rich zones (laihunite), and vacancy-free zones (fayalite) but do not assess their macroscopic distribution or abundance. Nor have previous studies directly measured the actual Fe^{3+}/ΣFe content of the phases involved.

To date, the best constraints on these issues come from indirect evidence. Schaefer (1983, 1985) presented results of Mössbauer studies of fayalite with a range of Fe^{3+} contents from four different localities with variable Fe^{3+}/Fe^{2+}. Mössbauer spectra and XRD patterns showed the presence of only a single phase with the olivine structure, so the presence of humite, hematite, or magnetite could be ruled out. Schaefer (1983, 1985) also noted that the XRD patterns became increasingly diffuse as the Fe^{3+} content of the Fa samples increased. Two sets of Mössbauer peaks exist at low temperatures: one octet corresponding to Fe^{2+} in "normal" olivine and two poorly resolved octets corresponding to Fe^{3+}-rich olivine. Because the spectra show no evidence of magnetic coupling that would be expected if Fe^{3+} and Fe^{2+} shared adjacent octahedra, she concluded that her samples con-

*E-mail: mddyar@amherst.edu

sisted of domains of fayalite and laihunite, intimately mixed on a very fine scale. SEM images suggested the presence of a two domain structure with domain sizes of at least 5 μm or more, and Schaefer hypothesized that these domains were intergrowths of the two end-member compositions. Estimates based on electron microprobe data are not reliable, and until now, there has been no analytical method capable of directly measuring Fe^{3+}/Fe^{2+} ratios at such a fine scale.

This study presents the first microscale analyses of Fe^{3+}/Fe^{2+} in Fe^{3+}-rich olivine using synchrotron micro-XANES, as described in Delaney et al. (1998). Because this technique provides accurate measurements of Fe^{3+}/Fe^{2+} at a scale of roughly 10×15 μm, it can be used to characterize the distribution of laihunite and fayalite at a scale comparable to that of the electron microprobe.

METHODS

Specimens are from Rockport, MA (0% $Fe^{3+}/\Sigma Fe$), Pantelleria, Italy (16%), Mourne Mountains, Ireland (32%), Qianan County, China (58%), and Lai-He Village (in northeastern China, the type locality for laihunite, 67%). Samples of the first four localities were taken from the same vials of powders used in the original work by Schaefer (1983, 1985) to allow direct comparison of results. Polished grain mounts were prepared and were used for both the SmX study and electron microprobe characterization. The latter technique was used to create backscatter images of the grains to help guide locations for SmX spots (Fig. 1), and to identify (and allow subsequent avoidance of) oxide inclusions that might affect SmX results.

Synchrotron micro-XANES (SmX) spectra were obtained using beam line x26a at the X-ray fluorescence microprobe facility, National Synchrotron Light Source (NSLS), Brookhaven National Laboratory. The structure of the Fe K absorption edge was scanned in the near edge region. Incident beam energies from 50 eV below the main absorption edge energy (7111 eV for Fe) to about 60 eV above the main edge were used. The beam was located by use of an oriented razor blade edge, so beam position could be constrained to within <5–15 μm. Using mutually orthogonal Kirkpatrick-Baez mirrors, the beam was focused to a 10×15 μm size. The X-ray sampling depth is probably large but >90% of the signal comes from the top 10 μm of the sample. Polished grains of the samples were mounted in epoxy on 25 mm lucite disks (standard electron microprobe mounts). The incident beam energy was controlled by a Si(III) channel cut monochromator. The incident X-ray energy was incremented by 0.3 eV intervals over the most critical energy range of -10 to +20 eV relative to the main absorption energy. This provides detailed mapping of the relationship between the pre-edge peak and the main absorption edge for comparison with the magnetite standard (see below) for which the pre-edge position is arbitrarily defined as 0.0 eV. Between -50 and -30 eV and above +30 eV, the X-ray energy was incremented by larger intervals to reduce data collection times. Each energy interval was counted between 5 and 20 live s (depending on the intensity of the main edge signal) for a total XANES spectrum acquisition time of about 20–30 min. Counting times were adjusted to obtain at least 10^5 counts per energy step at energies above the absorption edge. For additional details, see Delaney et al. (1996) and Bajt et al. (1994).

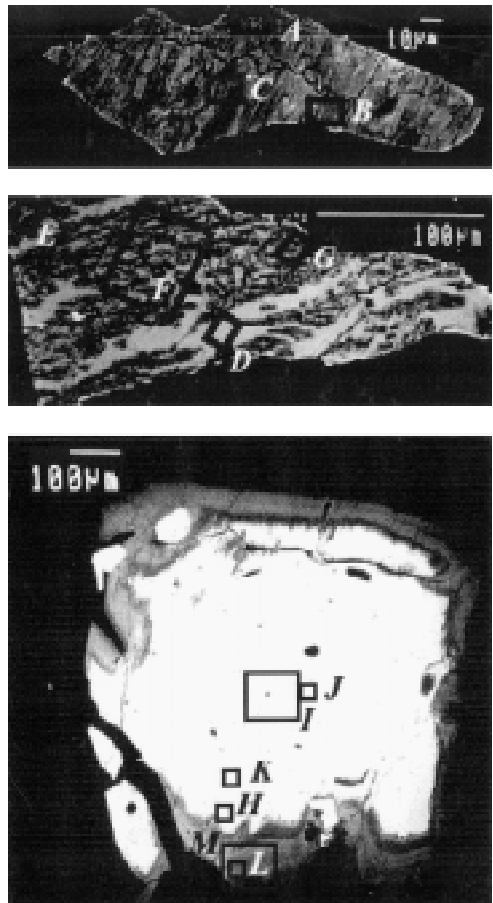The SmX technique uses systematic shifts in the Fe K-absorp-

FIGURE 1. Composite of electron microprobe backscatter images of grains analyzed from (**top**) Lai-He village, (**middle**) Mourne Mountains, and (**bottom**) Pantelleria. Boxes indicate the areas analyzed. Darker areas generally reflect lower Fe contents. Larger spots were from preliminary spectra analyzed in 1996. More recent spectra (1997–1998) with better focusing capabilities are from the smaller ~10×15 μm spots.

tion edge (the energy of a pre-edge peak is measured) that vary with oxidation state and coordination (bond strength of Fe-O). Calibration is made using the method of Bajt et al. (1994), which uses the pre-edge peak energies from synthetic fayalite (Fe_2SiO_4), natural magnetite (Fe_3O_4) obtained from the National Museum of Natural History (NMNH), and hematite (Fe_2O_3) to derive a calibration line for determining Fe^{3+} content from pre-edge energy. Pre-edge peak position for the spectrum of each unknown mineral is referenced to the pre-edge peak position of the magnetite spectra run before and after it:

$$\text{Position}^{\text{unknown}} = \text{Position}^{\text{unknown}}_{\text{measured}} - \text{Position}^{\text{magnetite}}_{\text{measured}}. \quad (1)$$

The regression (calibration) line is fit to the Fe^{3+} contents vs. pre-edge peak positions of fayalite, magnetite, and hematite in each session (and is therefore variable). For the most recent session at which olivine measurements were made, for example, the equation was of the form:

$$\%Fe^{3+} = 66.45 + 38.48\ \text{Position}^{\text{unknown}}. \quad (2)$$

This method has permitted successful measurements of $Fe^{3+}/\Sigma Fe$ in garnet, olivine, pyroxene, amphibole, micas, tourmaline, feldspar, and other minerals and glasses in an array of terrestrial materials (Delaney et al. 1998). Accuracy is believed to be ±5–10%.

RESULTS

Rockport

Of the five samples studied, only the Rockport fayalite proved to have homogeneous distribution of Fe^{3+}. These spectra (Fig. 1) differ little from those of the synthetic fayalite standard (not shown). Rockport fayalite is essentially completely reduced, with a measured $Fe^{3+}/\Sigma Fe$ of 3.1%.

Pantelleria

The Pantelleria sample is far more complex (Fig. 1c). At the center of the grain, the spectra (Fig. 2 and points I, J, K, and H in Fig. 1c) closely resembled that of the synthetic fayalite standard. Application of the regression line for that session gave a range for the core of $Fe^{3+}/\Sigma Fe$ from 3% to 12%. The lower Fe rim (clearly evident as a darker, laminated area in the backscatter image) is inferred to have $Fe^{3+}/\Sigma Fe$ of 35% on the inner portions (point M, Fig. 1) and 76% at the outermost edge (point L, Fig. 1). In the oxidized rim Fe is present as the laihunite component (possibly with a little hematite to account for the slightly high Fe^{3+}) and becomes all fayalite component over a distance of 5–100 µm. The shape of the main edge spectra for oxidized and unoxidized spots is the same; in Figure 2 both spectra have a pronounced sharp peak around 17 eV, which markedly differs from the rounded main edge peak shape of the magnetite spectrum shown at the bottom of Figure 2. Thus, there is no evidence to suggest a contribution from magnetite or an iron oxide phase to these spectra, so the rim is interpreted to be composed of gradational mixtures of a 0% Fe^{3+} (olivine) phase and a 67% Fe^{3+} (laihunite) phase. The value of 35% Fe^{3+} represents an area of laihunite mixed with olivine at a very fine scale, estimated to be <1 µm based on the size of the laminations visible in the backscatter images. Because the core is volumetrically large (~60% of the volume) relative to the rim, the overall bulk value of 16% Fe^{3+} obtained by Schaefer (1983, 1985) is very consistent with our results.

The oxidized rim of the Pantelleria sample suggests two possibilities for formation of the observed features, either of which is equally viable: (1) changing conditions during crystallization, or (2) post-crystallization reequilibration with an oxidizing fluid or magma. In the former case, a change in oxidizing conditions might have been brought on by changes in P, T, or f_{O_2} that occurred during mineral growth. In the latter scenario, some type of interaction with a fluid would have formed a diffusion front around the rim of the grains as the formerly reduced olivine re-equilibrated with a more oxidizing fluid or magma. This diffusion front is similar to what has been observed at HRTEM scales along grain boundaries and dislocations in metasomatized olivine (Banfield et al. 1990). Hematite decorations present along cracks in the sample (we did not analyze these areas with the XANES probe) further support the hypothesis that fayalite and O_2 react to form laihunite plus hematite:
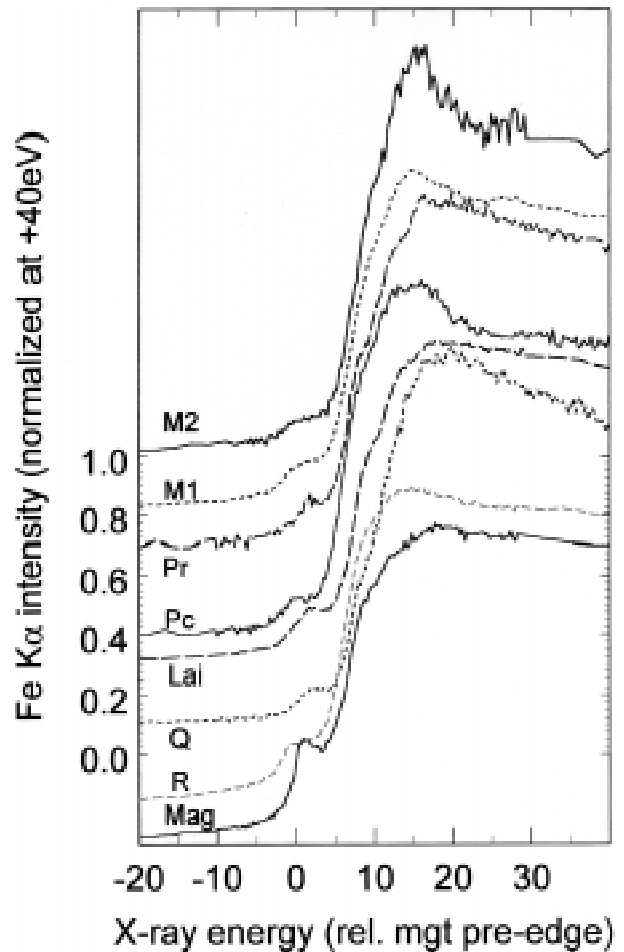

FIGURE 2. SmX spectra showing both the main edge (the dominant peak lying in the region above 10 eV) and pre-edge (peak at ~1.5 eV) of the XANES spectra of olivine from the Mourne Mountains (M1 is from point D in Fig. 1, M2 is point G), Pantelleria (Pr is point L in Fig. 1., PC is point J), the Lai-He village type locality for laihunite (Lai), Qianan (Q), and Rockport (R) with a magnetite (Mag and mgt) spectrum of the NMNH standard shown for comparison. All spectra are intensity normalized to a point 40 eV above the magnetite pre-edge and are displaced vertically for clarity. The overall increase in amplitude of pre-edge from top to bottom in the olivine samples (and their increasing similarity to the magnetite spectrum) may reflect an increasing contribution from an oxide phase. The main edge shape becomes less olivine-like in sequence from top to bottom.

$$2\ Fe_2^{2+}SiO_4 + \tfrac{3}{4}O_2 \rightarrow Fe^{2+}\square Fe_2^{3+}(SiO_4)_2 + \tfrac{1}{2}Fe_2O_3. \quad (3)$$

Iishi et al. (1997) suggest that such a breakdown reaction might occur via oxidation in an alkaline aqueous environment.

MOURNE MOUNTAINS

The Mourne Mountains sample is composed of fairly uniform, fine scale (~1–2 µm wide) intergrowths of bright and dark areas on the backscatter image (Fig. 1b), which produced different SmX spectra. We measured spectra of a few wider bands (20–30 µm) of

mostly dark (spectra taken at points F and G, Fig. 1, corresponding to 16% and 24% Fe^{3+}) or mostly bright material (points D and E, Fig. 1, corresponding to 29 and 34% Fe^{3+}). The difference in backscatter brightness between ~20% Fe^{3+} olivine and ~30% Fe^{3+} olivine is dramatic; these may represent subtle differences in populations of laihunite-rich and olivine-rich layers. Average values are again consistent within our error bars with the bulk $Fe^{3+}/\Sigma Fe$ value of 32% obtained by Schaefer (1983, 1985). The SmX spectra show no evidence for the presence of any phase other than olivine (Fig. 2). Based on our experience in other silicates, the presence of even tiny inclusions of hematite (100% Fe^{3+}) or magnetite (67% Fe^{3+}) can markedly alter both the pre-edge position and the main edge shape and there is no sign of any such contamination in the Mourne Mountains spectra.

The distribution of intergrowths in the Mourne Mountains sample is fundamentally different than in the Pantelleria sample. The observed texture is compatible with two possible mechanisms: (1) the formation of a two-phase aggregate via exsolution from a single homogeneous phase, and/or (2) high-temperature oxidation of olivine into oxidized olivine (e.g., Khisina et al. 1995). In the latter case, this texture may record the first stage oxidation measured by Khisina et al. (1995) at high temperatures. In either scenario, at the time of crystallization this grain may have had a composition representing a partial solid solution between laihunite and fayalite:

$$Fe^{2+}(Fe^{2+}_{3-3x}\square_x Fe^{3+}_{2x})(SiO_4)_4 \rightarrow Fe^{2+}\square Fe^{3+}_2(SiO_4)_2 + Fe^{2+}_2(SiO_4)_2. \quad (4)$$
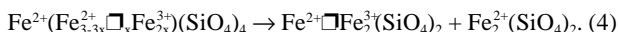
One implication is the existence of a stable high-temperature olivine with a composition representing fayalite-laihunite solid solution.

Qianan

The sample from Qianan is anomalous; its spectrum suggests an $Fe^{3+}/\Sigma Fe$ content of 90%, which is higher than even laihunite can be oxidized. The data are consistent with the presence of a very fine-scale intergrowth of hematite, silica, and laihunite. This grain may be showing the complete breakdown of laihunite to hematite + amorphous silica, as was observed by Iishi et al. (1997) for alteration of laihunite in an acidic aqueous environment. If the reaction

$$2Fe^{2+}\square Fe^{3+}_2(SiO_4)_2 + {}^1/_2O_2 \rightarrow 3Fe_2O_3 + 4SiO_2 \quad (5)$$
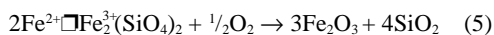
is taking place, then the abundance of hematite would have to be greater than the abundance of laihunite to generate the 90% Fe^{3+} in the area analyzed. However, if reaction 3 is occurring here, then fayalite would be a minor constituent relative to hematite. These two hypotheses could probably be distinguished by TEM. The sharpness of the main edge in the XANES spectrum of the grain we analyzed (Fig. 2) is distinct from the rounded magnetite main edge, and the Qianan pre-edge position is markedly different from the magnetite pre-edge (which is more intense because of the contribution of Fe^{3+} in a less symmetrical tetrahedral site). This suggests the presence of only octahedral Fe^{3+}, so it does not discriminate between reactions 3 and 5, and may suggest the presence of either hematite only or a mixture of hematite + olivine. Note that Schaefer (1983) did not observe any contribution from

hematite in her Mössbauer spectra (though the particle size may have been too small to see it).

Lai-He Village

Two grains of a sample from the laihunite type locality were analyzed, one of which is shown in Figure 1c. Similar to the Mourne Mountains sample, this grain displays uniformly distributed 1–3 μm light and dark regions in backscatter. The scale of Fe^{3+} variation is smaller than our SmX beam. The mottling that is evident in the backscatter image strongly suggests that this is a two-phase system, although it is probably exsolved from a single phase. Therefore the Fe^{3+} contents measured by our 10×15 μm beam are an average of light and dark regions, which may represent only subtle variations in Fe^{3+} contents and not the two end-member phases. If the light and dark regions are interpreted to represent fayalite (0% Fe^{3+}) and laihunite (67% Fe^{3+}), respectively, then the total %Fe^{3+} would be 33% if the areas are equal volumetrically. Such an interpretation would be inconsistent with the bulk $Fe^{3+}/\Sigma Fe$ for this sample, which is 67% (based on Mössbauer spectra) and with the SmX results (two spots with 69 and 71% Fe^{3+}).

However, AEM work by Kitamura et al. (1984) on samples from the same locality found that laihunite intergrowths into fayalite that appear to be chemically homogeneous at a 2 μm scale are actually mixtures of laihunite and magnetite. They hypothesized the following reaction:

$$6Fe^{2+}_2 SiO_4 + 2O_2 \rightarrow 3 \, Fe^{2+}\square Fe^{3+}_2(SiO_4)_2 + Fe_3O_4. \quad (6)$$
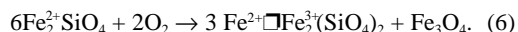
But they also noted that they could induce breakdown to fayalite + hematite by prolonged exposure to the electron beam:

$$Fe^{2+}\square Fe^{3+}_2(SiO_4)_2 + Fe_3O_4 \rightarrow 2Fe^{2+}_2 SiO_4 + Fe_2O_3 + {}^1/_2O_2. \quad (7)$$
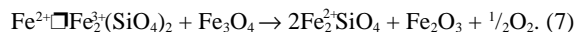
Schaefer (1983) did not see any contribution from magnetite or hematite in her Mössbauer spectra, but these phases would have to be either superparamagnetic (i.e., of a very small grain size, such that magnetic splitting is not present in the Mössbauer spectra) and/or be present in amounts greater than 1 mol% to be detected. In our XANES spectra of the sample from Lai-He, the pre-edge intensity is increased relative to a spectrum of clean fayalite (as would be the case if Fe^{3+} is present in tetrahedral coordination, as it is in magnetite; see Fig. 2), and the overall shape of the main edge in our laihunite spectra is similar to that of magnetite. Therefore, the XANES data favor reaction 4, consistent with the AEM results. In fact, the light and dark areas of the grains may well correspond to magnetite-rich areas alternating with laihunite. Both would have the same $Fe^{3+}/\Sigma Fe$, but they would appear different in a backscatter image due to their different total Fe contents.

DISCUSSION

SmX measurements of these samples were performed on a 10 μm × 15 μm scale that is significantly larger than TEM but much smaller than that of bulk measurements. As such, we can place spatial constraints on the oxidation present in the samples studied here. Our results show that the effects of oxidation in olivine can be either macroscopic or submicroscopic. Pantelleria olivine contains a reduced core roughly 700 μm in size, with an oxidized rim ~100 μm in size that is 100% laihunite on the outermost rim. Oli-

vine from the Mourne Mountains shows fine (1–3 μm) and coarse (20–30 μm) banding of light and dark areas in backscatter images with distinct $Fe^{3+}/\Sigma Fe$ contents of 20 and 30%, respectively. Laihunite from the type locality is also two phase (and possibly three phase if magnetite is present), again at a scale of less than 1–3 μm. Because our work was done on single grains, we can only hypothesize the mechanisms that generate these distributions. Clearly, there is a need for further SmX studies of these samples based on analyses of thin sections so that textural observations can be placed into better petrologic context.

ACKNOWLEDGMENTS

REFERENCES CITED

Bajt, S., Sutton, S.R., and Delaney, J.S. (1994) Microanalysis of iron oxidation states in silicates and oxides using X-ray absorption near edge structure (XANES). Geochimica et Cosmochimica Acta, 58, 5209–5214.

Banfield, J.F., Veblen, D.R., and Jones, F. (1990) Transmission electron microscopy of subsolidus oxidation and weathering of olivine. Contributions to Mineralogy and Petrology, 106, 110–123.

Banfield, J.F., Dyar, M.D., and McGuire, A.V. (1992) The defect microstructure of oxidized mantle olivine from Dish Hill, California. American Mineralogist, 77, 977–986.

Delaney, J.S., Dyar, M.D., Sutton, S.R., and Bajt, S. (1998) Redox ratios with relevant resolution: Solving an old problem by using the synchrotron microXANES probe. Geology, 26, 139–142.

Ferrifayalite Research Group (Department of Geology of the Peking University, Institute of Geology and Mineral Resources of the Chinese Academy of Geological Sciences) (1976) Ferrifayalite and its crystal structure. Acta Geologica Sinica, 2, 160–175 (in Chinese).

Ginsburg, I.V., Lisitsina, G.A., Sadikova, A.T., and Sidorenko, G.A. (1962) Fayalite of granite rocks and the products of its alteration (Kuraminskii Range, Central Asia). Akademiya Nauk CCCP, Trudy Mineralogicheskogo Museya, 13, 16–42 (in Russian).

Iishi, K., Kadomi, M., and Okamoto, K. (1989a) Synthesis of laihunite by heating Fe-Mn olivine in air. Neues Jahrbuch für Mineralogie Monatshefte, 6, 245–254.

Iishi, K., Okamoto, K., and Kadomi, M. (1989b) Formation of laihunite from Fe-(Mg, Co, Mn, Ca) olivines. Neues Jahrbuch für Mineralogie Monatshefte, 8, 345–356.

Iishi, K., Torigoe, K., and Han, X.J. (1997) Oriented precipitate complexes in iron-rich olivines produced experimentally in aqueous oxidizing environment. Physics and Chemistry of Minerals, 25, 8–14.

Janney, D.E. and Banfield, J.F. (1998) Distribution of cations and vacancies and the structure of defects in oxidized intermediate olivine by atomic-resolution transmission electron microscopy and image simulation. American Mineralogist, 83, 799–810.

Khisina, N.R., Khramov, D.A., Kolosov, M.V., Kleschev, A.A., and Taylor, L.A. (1995) Formation of ferriolivine and magnesioferrite in Mg-Fe olivine. Physics and Chemistry of Minerals, 22, 241–250.

Khisina, N.R., Khramov, D.A., Kleschev, A.A., and Rusakov, V.S. (1996) Mössbauer spectroscopy data on oxidation kinetics of Mg-Fe olivine. Physics and Chemistry of Minerals, 23, 284.

Kitamura, M., Shen, B., Banno, S., and Morimoto, N. (1984) Fine textures of laihunite, a nonstoichiometric distorted olivine-type material. American Mineralogist, 69, 154–160.

Kondoh, S., Kitamura, M., and Morimoto, N. (1985) Synthetic laihunite ($\square_x Fe^{2+}_{2-3x} Fe^{3+}_{2x} SiO_4$), an oxidation product of olivine. American Mineralogist, 70, 737–746.

Nikitin, V.D. (1934) A new variety of mineral of the olivine group. Zapiski Vserossiyskogo Mineralogiyeskogo Obvestva, seriya 2, ch. 65, 1–2, 281–288 (in Russian).

Schaefer, M.W. (1983) Measurements of iron(III)-rich fayalites. Nature, 303, 325–327.

———(1985) Site occupancy and two-phase character of "ferrifayalite". American Mineralogist, 70, 729–736.

Shen, B., Tamada, O., Kitamura, M., and Morimoto, N. (1986) Superstructure of laihunite-3M ($\square_{0.40} Fe^{2+}_{0.80} Fe^{3+}_{0.80} SiO_4$). American Mineralogist, 71, 1455–1460.

Tamada, O., Shen, B., and Morimoto, N. (1983) The crystal structure of laihunite ($\square_{0.40} Fe^{2+}_{0.80} Fe^{3+}_{0.80} SiO_4$)-non-stoichiometric olivine-type mineral. Mineralogical Journal, 11, 382–391.